Basis Set and Density Functional Dependence of Vibrational Raman Optical Activity Calculations

Markus Reiher*,†

Lehrstuhl für Theoretische Chemie, Universität Bonn, Wegelerstrasse 12, D-53115 Bonn, Germany

Vincent Liégeois‡ and Kenneth Ruud*

Department of Chemistry, University of Tromsø, N-9037 Tromsø, Norway

Received: April 24, 2005; In Final Form: July 3, 2005

We present an extensive investigation of the dependence of the scattering intensity difference of right and left circularly polarized light observed in vibrational Raman optical activity (VROA) on the choice of basis set and exchange-correlation functional. These dependencies are investigated for five molecules for which accurate experimental data are available: (*S*)-methyloxirane, (*R*)-epichlorhydrin, (*S*)-glycidol, (*M*)-spiro[2,2]-pentane-1,4-diene, and (*M*)-σ-[4]-helicene. Calculations are presented using the SVWN exchange-correlation functional (LDA), the BLYP exchange-correlation functional, and the B3LYP hybrid functional, using six different basis sets: the cc-pVDZ, cc-pVTZ, aug-cc-pVDZ, aug-cc-pVTZ, Sadlej's polarized basis set, and a minimal VROA basis set recently proposed by Zuber and Hug. It is demonstrated that results from pure gradient-corrected and hybrid functionals are comparable and that the aug-cc-pVDZ and aug-cc-pVTZ basis sets yield similar results. Furthermore, the combination of the small basis set by Zuber and Hug with an accurate force field represents the best compromise between computational accuracy and computational efficiency.

I. Introduction

In the late 1960s, Barron and Buckingham derived a formalism for the study of the vibrational Raman effect using circularly polarized light and, in particular, the difference in scattering intensities for left and right circularly polarized light.[1] They found that for chiral molecules there would be a difference in the scattering intensity for left and right circularly polarized light and named the technique vibrational Raman optical activity (VROA). Later, Barron, Bogaard, and Buckingham demonstrated the existence of VROA experimentally,[2] an observation independently confirmed by Hug et al.,[3] and the field has been growing steadily since then. However, the difference between the scattering intensities of left and right circularly polarized light is 5 orders of magnitude smaller than ordinary Raman intensities, requiring very sensitive experimental equipment.[4,5]

The ab initio calculation of VROA is still in its infancy, despite its potential importance. The first calculation of the circular intensity differences observed in VROA spectroscopy was presented by Polavarapu and co-workers as recently as 1990[6] using finite numerical differentiation of Hartree−Fock (HF) linear response functions calculated in the static limit. These calculations were gauge-origin dependent. A gauge-origin independent and frequency-dependent approach to the calculation of VROA scattering intensity differences between left and right circularly polarized light for HF and multiconfigurational self-consistent field calculations (MCSCF) was presented by Helgaker et al. in 1994,[7] in which the gauge-origin independence was ensured through the use of London atomic orbitals.[8] This approach was recently extended to also allow for frequency-dependent and gauge-origin independent calculations using density-functional theory (DFT).[9−11]

In recent years an increasing number of theoretical studies of VROA spectra have been appearing; see refs 12−15 for an account of recent theoretical studies. However, compared to the explosive growth in the theoretical calculation of optical rotation (see refs 16−18 for some recent reviews), which use some of the same second-order quantities that are of interest also for VROA calculations, VROA calculations remain limited to small molecules and often restricted to calculations at the Hartree−Fock level of theory using MP2 or DFT force fields.

Very few systematic studies of the computational requirements for VROA intensities differences exist. This is to a large extent due to the problems associated with reaching near basis set limit results for larger molecules. However, a very detailed study of the basis set requirements of VROA calculations was presented by Zuber and Hug[19] who also proposed a minimal basis set which gives close to aug-cc-pVDZ results. No studies of the importance of the choice of DFT functional have to our knowledge been presented to date.

In this work, we rectify the situation with a detailed study of the basis set requirements and we also analyze the importance of the choice of exchange-correlation functional in density functional theory calculations. To accomplish this task, a set of five molecules has been selected: (*S*)-methyloxirane (**1**), (*R*)-epichlorhydrin (**2**), (*S*)-glycidol (**3**), (*M*)-spiro[2,2]pentane-1,4-diene (**4**), and (*M*)-σ-[4]-helicene (**5**) (see Figure 1). For these

* To whom correspondence should be addressed. E-mail: Kenneth.Ruud@chem.uit.no; markus.reiher@uni-jena.de.

† Present address: Institut für Physikalische Chemie, Universität Jena, Helmholtzweg 4, D-07743 Jena, Germany.

‡ Permanent address: Laboratoire de Chimie Théorique Appliquée, Facultés Universitaires Notre-Dame de la Paix (FUNDP), Rue de Bruxelles 61, B-5000 Namur, Belgium.

10.1021/jp052123h CCC: $30.25
Published on Web 07/30/2005

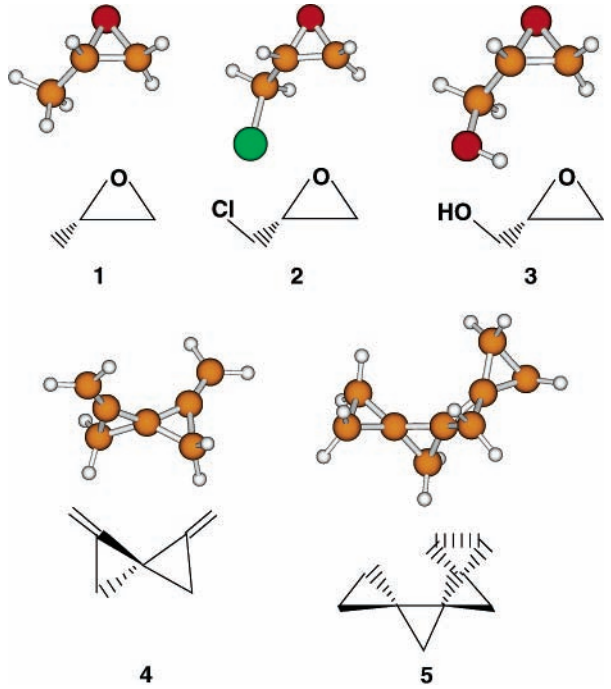

Figure 1. Optimized molecular structures for (*S*)-methyloxirane (**1**), (*R*)-epichlorhydrin (**2**), (*S*)-glycidol (**3**), (*M*)-spiro[2,2]pentane-1,4-diene (**4**), and (*M*)-*σ*-[4]-helicene (**5**).

molecules, recent, highly accurate, experimental data are available to which we can compare our results.[20,21]

This paper is organized as follows: In section II, we briefly give the necessary theoretical background for understanding which molecular quantities contribute to the VROA intensity differences. Section III gives the computational details for our calculations, and section IV presents the results. In section V, we compare simulated VROA spectra based on our best theoretical results with experimentally recorded spectra for the three molecules with only a single conformation **1**, **4**, and **5**. In section VI we give some concluding remarks.

II. Theoretical Background

As shown by Barron and Buckingham,[1] the scattering intensity differences between right and left circularly polarized light are determined (within the Placzek approximation[22]) by the geometrical derivatives of the electric-dipole/electric-dipole polarizability

$$\alpha_{\alpha\beta} = 2\sum_{n\neq 0}\omega_{n0}\frac{Re[\langle 0|\mu_\alpha|n\rangle\langle n|\mu_\beta|0\rangle]}{{\omega_{n0}}^2-\omega^2} \tag{1}$$

with the electric-dipole operator

$$\mu_\alpha = -\sum_i r_{i\alpha}; \qquad \alpha\in\{x,y,z\} \tag{2}$$

the electric-dipole/magnetic-dipole polarizability

$$G'_{\alpha\beta} = -2\omega\sum_{n\neq 0}\frac{Im[\langle 0|\mu_\alpha|n\rangle\langle n|m_\beta|0\rangle]}{{\omega_{n0}}^2-\omega^2} \tag{3}$$

with the magnetic-dipole operator

$$m_\beta = -\frac{1}{2}\sum_i l_{i\beta}; \qquad \beta\in\{x,y,z\} \tag{4}$$

and the electric-dipole/electric-quadrupole polarizability

$$A_{\alpha\beta\gamma} = 2\sum_{n\neq 0}\omega_{n0}\frac{Re[\langle 0|\mu_\alpha|n\rangle\langle n|\Theta_{\beta\gamma}|0\rangle]}{{\omega_{n0}}^2-\omega^2} \tag{5}$$

with the electric-quadrupole operator

$$\Theta_{\beta\gamma} = -\frac{1}{2}\sum_i [3r_{i\beta}r_{i\gamma} - r_i^2\delta_{\beta\gamma}]; \qquad \beta,\gamma\in\{x,y,z\} \tag{6}$$

In these sum-over-states formulas, the summation is taken over all excited states and atomic units are used throughout. The operator definitions contain elements of the position r_i and angular momentum l_i operators for electron i. In the equations, ω denotes the incident laser beam frequency and ω_{n0} the excitation energy from the ground state $|0\rangle$ to the nth excited state $|n\rangle$. As the magnetic-dipole moment in the electric-dipole/magnetic-dipole polarizability gives rise to an artificial gauge-origin dependence in ab initio calculations employing finite basis sets,[23] we use London atomic orbitals to ensure that our calculated results are independent of the choice of gauge origin also with the finite basis sets used in our calculations.[7,9]

Using these property tensors, we calculate the backscattering (180°) intensity difference as[24]

$$I^R(180°) - I^L(180°) = \frac{1}{c}(24\beta(G')^2 + 8\beta(A)^2) \tag{7}$$

with the speed of light c and the isotropic and anisotropic invariants of the property tensors

$$\alpha = \frac{1}{3}\alpha_{\alpha\alpha} \tag{8}$$

$$\beta(\alpha)^2 = \frac{1}{2}(3\alpha_{\alpha\beta}\alpha_{\alpha\beta} - \alpha_{\alpha\alpha}\alpha_{\beta\beta}) \tag{9}$$

$$\beta(G')^2 = \frac{1}{2}(3\alpha_{\alpha\beta}G'_{\alpha\beta} - \alpha_{\alpha\alpha}G'_{\beta\beta}) \tag{10}$$

$$\beta(A)^2 = \frac{1}{2}\omega\alpha_{\alpha\beta}\epsilon_{\alpha\gamma\delta}A_{\gamma\delta\beta} \tag{11}$$

(note that implicit summation over repeated indices has been used). $\epsilon_{\alpha\gamma\delta}$ is the unit third-rank antisymmetric tensor.

For the vibrational Raman scattering process, we need the vibrational transition moments, whose geometry dependence is as usual approximated by a truncated Taylor series expansion around the equilibrium geometry r_e[24]

$$\langle\nu_{0p}|\alpha_{\alpha\beta}|\nu_{1p}\rangle\langle\nu_{1p}|\alpha_{\alpha\beta}|\nu_{0p}\rangle = \frac{1}{2\omega_p}\left(\frac{\partial\alpha_{\alpha\beta}}{\partial Q_p}\right)_e\left(\frac{\partial\alpha_{\alpha\beta}}{\partial Q_p}\right)_e \tag{12}$$

$$\langle\nu_{0p}|\alpha_{\alpha\beta}|\nu_{1p}\rangle\langle\nu_{1p}|G'_{\alpha\beta}|\nu_{0p}\rangle = \frac{1}{2\omega_p}\left(\frac{\partial\alpha_{\alpha\beta}}{\partial Q_p}\right)_e\left(\frac{\partial G'_{\alpha\beta}}{\partial Q_p}\right)_e \tag{13}$$

$$\langle\nu_{0p}|\alpha_{\alpha\beta}|\nu_{1p}\rangle\langle\nu_{1p}|\epsilon_{\alpha\gamma\delta}A_{\gamma\delta\beta}|\nu_{0p}\rangle = \frac{1}{2\omega_p}\left(\frac{\partial\alpha_{\alpha\beta}}{\partial Q_p}\right)_e\left(\frac{\partial\epsilon_{\alpha\gamma\delta}A_{\gamma\delta\beta}}{\partial Q_p}\right)_e \tag{14}$$

with the vibrational ground state and first excited-state wave

functions ν_{0p} and ν_{1p}, respectively, for mode p and the corresponding normal coordinate Q_p and harmonic frequency ω_p.

To analyze the wealth of computational data which results from calculating the different property tensors, their derivatives with respect to normal coordinates, and the intensity differences between the right and left circularly polarized scattered light, we adopt the strategy of Zuber and Hug:[19] For each molecule, basis set, and functional we calculate the quantity

$$\delta(I) = \frac{\sum_p |I_p^{\text{trial}} - I_p^{\text{ref}}|}{\sum_p |I_p^{\text{ref}}|} \tag{15}$$

where I_p^{trial} and I_p^{ref} refer to the intensity differences of the computational method being evaluated and the reference computational method, respectively. The summations run over all vibrational modes of the molecule, and we do not distinguish between any different kind of vibrational modes. In addition, we report the number of modes for which there is a difference in sign with respect to the reference intensity differences. A large number of modes of a different sign but a small $\delta(I)$ value thus predominantly calculate an incorrect sign for weak vibrational intensity differences, whereas a small number of vibrational modes with opposite sign but a large $\delta(I)$ value indicate that some strong intensity differences are incorrectly predicted. Let us note, however, that differences in the force fields may lead to a different ordering of the vibrational modes, giving rise to apparent differences in the sign of the intensity differences as well as artificially large $\delta(I)$ values. Due to the large amount of data collected, we have not made any attempts at analyzing the individual modes to avoid such apparently incorrect ordering of the vibrational bands, including instead these deviations directly in our reported number of incorrect signs and $\delta(I)$ values. All the output files from the calculations can be downloaded from our website http://www.ipc.uni-jena.de/reiher/vroa.html.

III. Computational Details

Three different exchange-correlation functionals will be investigated: the Slater−Vosko−Wilk−Nusair exchange-correlation functional,[25,26] the generalized-gradient functional BLYP, using Becke's 1988 exchange functional[27] with the Lee, Yang, and Parr correlation functional,[28] and finally the hybrid functional B3LYP using Becke's three-parameter hybrid-exchange functional[29] with the LYP correlation functional.[28] We employ Dunning's cc-pVDZ, aug-cc-pVDZ, cc-pVTZ, and aug-cc-pVTZ basis sets,[30,31] as well as the basis set introduced by Sadlej.[32,33] Following Zuber and Hug,[19] we also augment a 3-21++G basis set[34] by one diffuse p-type polarization function with a coefficient $\zeta = 0.2$ for each hydrogen atom in order to reduce the computational effort for the property tensor calculations.

Determining the reference intensity differences is a difficult problem. It is difficult to extract these data directly from the experimental data due to the overlapping of vibrational bands and the problems in determining the integration range for calculating the total scattering cross sections. These problems would remain also if we considered the relative intensity differences, as the band shapes of the VROA and Raman bands might be different, thus causing inaccuracies in the experimentally derived quantities. For this reason, we will use as our reference value both the aug-cc-pVTZ basis set result using the same exchange-correlation functional, as well as the B3LYP/aug-cc-pVTZ results, with the exception of (*M*)-σ-[4]-helicene, where the aug-cc-pVDZ results will be used as reference values since Dunning's triple-ζ basis sets required computer resources for this molecule beyond reasonable effort. We will instead compare directly the B3LYP/aug-cc-pVTZ predicted spectra with the experimental data of refs 20 and 21 to judge the quality of these reference data.

Here we will only consider the scattering intensity differences. The scattering intensity differences are of course intimately connected to the quality of the force field through the transformation to the normal coordinates,[7,24,35,36] and thus the results obtained for the intensity differences may as much reflect the quality of the force field as the quality of the intensity differences. This has also been utilized as a means to speed up the calculation of VROA spectra.[9,20,37] However, we will here almost exclusively consider the calculated intensity differences and force fields as calculated at a uniform level of approximation, that is, the property tensors and the force field are calculated with the same basis set. The only exception to this is the basis set of Zuber and Hug, which clearly will be too small to provide accurate force fields, yet it is at the same time small enough that it will allow for VROA studies of very large molecules. For this reason we will, in addition to the data for this basis set, also present data when this basis set is used together with the aug-cc-pVTZ force field (aug-cc-pVDZ for (*M*)-σ-[4]-helicene) using the same exchange-correlation functional, to see if this basis can be combined with an accurate force field to give reliable intensity differences for large molecules.

The above-mentioned generalized polarizabilities are available from the Dalton program[38] both at the HF/MCSCF[7] and at the DFT level[9] of theory. Due to the presence of the geometrical derivatives and the magnetic-dipole-moment operator defined using London atomic orbitals,[39] the implementation of analytical third derivatives for these generalized tensors represents a challenging task, and one is therefore, in practice, forced to employ schemes using numerical derivatives with respect to the geometrical distortions.

In the calculation of geometrical derivatives of molecular properties using a numerical scheme, one is faced with the high computational scaling of the approach since there will be a need for at least 6*N* property calculations for a molecule containing *N* atoms. Since even a single-point calculation of a higher-order molecular property may be rather time consuming, the additional 6*N* property calculations needed may render the determination of the geometrical derivatives of these properties virtually impossible. This is particularly important for properties such as those determining the scattering intensity differences observed in VROA, since they occur for chiral molecules, and the chiral molecules are often quite large and in most cases do not possess any molecular symmetry that could otherwise have been used to reduce the computational cost.

All calculations reported in this paper have been obtained using parallel software on loosly coupled computer clusters. Two different approaches have been employed. For some of the molecules, the VROA scattering intensity differences have been obtained using a parallel version of the Dalton quantum chemistry program,[38] in which the calculation of two-electron integrals, the numerical integration in the evaluation of exchange-correlation energies and potentials, and the generation of numerical grids have been parallelized following earlier implementations.[40,41]

In other cases, the evaluation of the VROA intensities have been done using the SNF program,[42] for which a new interface for the collection of property tensors at displaced structures has been implemented. The SNF program distributes the different

distorted molecular geometries that are needed for the evaluation of the numerical derivatives of the second-order molecular properties to different compute nodes. Dalton is then executed for each distorted geometry sent to each compute node. At the end of the calculation, the data calculated for all the distorted geometries are analyzed in order to obtain the intensity differences from finite-difference derivatives with respect to the nuclear coordinates. In all cases, the calculated force fields have been obtained as numerical first derivatives of analytically calculated molecular gradients. A step length of 0.01 bohr has been used in the numerical differentiation, and the response vectors have been converged to a threshold of 5×10^{-5} with respect to the norm of the response vector. The numerical force field has been shown to give results that deviate at most by 2 cm^{-1}, usually by less than 1 cm^{-1}, from those obtained using analytical force fields.

While the Dalton program allows one to use the parallel mode of Dalton for the consecutive evaluation of displaced structures, the SNF program allows a parallel evaluation of the displaced structures running Dalton in serial mode. In view of the computational effort for the present study, this strategy allows us to use computer resources in the most optimal way. Furthermore, this interface allows us to easily extend our calculations using mode selection to target specific vibrational modes of large molecular complexes,[43,44] and work along these lines is in progress.

IV. Results and Discussion

For the calculation of $\delta(I)$, we used the aug-cc-pVTZ basis set and always the same functional as reference method. In addition, we compared the intensity differences obtained with LDA and BLYP via $\delta(I)$ with B3LYP/aug-cc-pVTZ as the reference. (Note that for the largest molecule, that is, for the helicene **5**, we always used the aug-cc-pVDZ basis set as reference.)

The results for methyloxirane **1** show that the Zuber & Hug and cc-pVDZ basis sets yield the largest $\delta(I)$ values and also the largest number of wrong signs when compared with the aug-cc-pVTZ basis set using the same functional (see Table 1).

The Sadlej and cc-pVTZ basis sets yield improved results, but the best agreement with the aug-cc-pVTZ reference scattering intensity differences is obtained with the aug-cc-pVDZ basis set. Also the small Zuber & Hug basis set in combination with the aug-cc-pVTZ force field yields remarkably good results. The comparison of the LDA and BLYP data with the B3LYP/aug-cc-pVTZ reference demonstrates that the LDA data deviates the most, while in the case of the BLYP functional, the number of wrong signs is comparatively small for all basis sets and also the $\delta(I)$ values are quite small. However, significant deviations occur also for the largest basis sets aug-cc-pVDZ and aug-cc-pVTZ in combination with the LDA and BLYP functionals.

The epichlorhydrine molecule **2** possesses the same number of normal modes as methyloxirane **1** but some modes involve the motion of the chlorine atom, which substitutes a hydrogen atom in the methyl group of **1**. The general picture is thus similar for **1** and **2** (see Table 2).

However, there are important differences. When LDA and BLYP are compared with the B3LYP/aug-cc-pVTZ reference, larger deviations with respect to the number of wrong signs occur for most functional/basis-set combinations. Exceptions are the BLYP/Sadlej and BLYP/aug-cc-pVDZ (and also to a certain degree the LDA/aug-cc-pVDZ and LDA/aug-cc-pVTZ combinations). These two computational models do not show a single wrong sign and also have a small $\delta(I)$ value. For **2**, the Zuber & Hug basis set with a high-quality force field (aug-cc-pVTZ) performs less satisfactory than the aug-cc-pVDZ data, both when the B3LYP/aug-cc-pVTZ results are used as a

TABLE 1: Comparison of the Calculated Intensity Differences for Left and Right Circularly Polarized Light for the Different Basis Sets and Functionals for 1[a]

		functional/ aug-cc-pVTZ		comparison to B3LYP/ aug-cc-pVTZ	
functional	basis set	$\delta(I)$	no. of wrong signs	$\delta(I)$	no. of wrong signs
LDA	3-21++G(p)[b]	2.020	10	1.844	7
	3-21++G(p)[b,c]	0.536	6	1.049	1
	Sadlej	0.276	2	1.040	5
	cc-pVDZ	1.108	4	1.706	5
	cc-pVTZ	0.343	3	1.247	6
	aug-cc-pVDZ	0.178	0	1.052	5
	aug-cc-pVTZ			1.011	5
BLYP	3-21++G(p)[b]	1.009	6	1.265	6
	3-21++G(p)[b,d]	0.457	2	0.419	2
	Sadlej	0.949	2	1.091	2
	cc-pVDZ	1.241	6	1.486	4
	cc-pVTZ	0.882	4	0.958	2
	aug-cc-pVDZ	0.189	2	0.811	2
	aug-cc-pVTZ			0.612	2
B3LYP	3-21++G(p)[b]	1.175	6		
	3-21++G(p)[b,e]	0.436	1		
	Sadlej	0.947	2		
	cc-pVDZ	1.371	5		
	cc-pVTZ	0.485	2		
	aug-cc-pVDZ	0.226	2		

[a] Total number of vibrational modes is 24. For an explanation of the different quantities, see text. [b] Using a single polarization function with exponent 0.2 for hydrogens only, as suggested by Zuber and Hug.[19] [c] Using the LDA/aug-cc-pVTZ force field, see text. [d] Using the BLYP/aug-cc-pVTZ force field, see text. [e] Using the B3LYP/aug-cc-pVTZ force field, see text.

TABLE 2: Comparison of the Calculated Intensity Differences for Left and Right Circularly Polarized Light for the Different Basis Sets and Functionals for 2[a]

		functional/ aug-cc-pVTZ		comparison to B3LYP/ aug-cc-pVTZ	
functional	basis set	$\delta(I)$	no. of wrong signs	$\delta(I)$	no. of wrong signs
LDA	3-21++G(p)[b]	0.693	7	0.965	9
	3-21++G(p)[b,c]	0.493	3	0.730	7
	Sadlej	0.302	2	0.829	6
	cc-pVDZ	0.846	4	1.511	8
	cc-pVTZ	0.283	3	0.827	7
	aug-cc-pVDZ	0.080	0	0.494	4
	aug-cc-pVTZ			0.495	4
BLYP	3-21++G(p)[b]	0.730	7	0.838	8
	3-21++G(p)[b,d]	0.450	3	0.515	6
	Sadlej	0.306	3	0.306	0
	cc-pVDZ	0.749	9	0.855	8
	cc-pVTZ	0.195	2	0.317	5
	aug-cc-pVDZ	0.203	3	0.262	0
	aug-cc-pVTZ			0.213	3
B3LYP	3-21++G(p)[b]	0.721	10		
	3-21++G(p)[b,e]	0.392	4		
	Sadlej	0.436	1		
	cc-pVDZ	0.606	3		
	cc-pVTZ	0.211	1		
	aug-cc-pVDZ	0.169	0		

[a] Total number of vibrational modes is 24. For an explanation of the different quantities, see text. [b] Using a single polarization function with exponent 0.2 for hydrogens only, as suggested by Zuber and Hug.[19] [c] Using the LDA/aug-cc-pVTZ force field, see text. [d] Using the BLYP/aug-cc-pVTZ force field, see text. [e] Using the B3LYP/aug-cc-pVTZ force field, see text.

TABLE 3: Comparison of the Calculated Intensity Differences for Left and Right Circularly Polarized Light for the Different Basis Sets and Functionals for 3[a]

		functional/ aug-cc-pVTZ		comparison to B3LYP/ aug-cc-pVTZ	
functional	basis set	$\delta(I)$	no. of wrong signs	$\delta(I)$	no. of wrong signs
LDA	3-21++G(p)[b]	1.257	10	1.030	7
	3-21++G(p)[b,c]	0.505	3	0.839	6
	Sadlej	0.448	4	0.492	5
	cc-pVDZ	0.807	6	0.963	7
	cc-pVTZ	0.321	2	0.824	7
	aug-cc-pVDZ	0.282	3	0.707	6
	aug-cc-pVTZ			0.600	7
BLYP	3-21++G(p)[b]	1.293	12	1.266	10
	3-21++G(p)[b,d]	0.526	5	0.602	7
	Sadlej	0.691	4	0.686	4
	cc-pVDZ	0.937	9	0.988	7
	cc-pVTZ	0.333	5	0.589	7
	aug-cc-pVDZ	0.438	6	0.507	6
	aug-cc-pVTZ			0.315	4
B3LYP	3-21++G(p)[b]	1.090	9		
	3-21++G(p)[b,e]	0.384	5		
	Sadlej	0.473	4		
	cc-pVDZ	0.568	5		
	cc-pVTZ	0.295	2		
	aug-cc-pVDZ	0.420	3		

[a] Total number of vibrational modes is 27. For an explanation of the different quantities, see text. [b] Using a single polarization function with exponent 0.2 for hydrogens only, as suggested by Zuber and Hug.[19] [c] Using the LDA/aug-cc-pVTZ force field, see text. [d] Using the BLYP/aug-cc-pVTZ force field, see text. [e] Using the B3LYP/aug-cc-pVTZ force field, see text.

reference and when the aug-cc-pVTZ basis set with the same functional is used as a reference. It is furthermore interesting to note that the $\delta(I)$ values are in general smaller for **2** than those for **1**.

The results for glycidol **3** show the same trends as already noted for **1**—apart from the fact that the number of wrong signs is now slightly larger for each entry, which may be due to the larger total number of normal modes (compare Table 3). In particular, the Zuber & Hug basis set with a high-quality force field performs as good as the aug-cc-pVDZ (independent of the reference method).

Coming to the larger molecules of different structure, we note that the spiro compound **4** possesses more normal modes but not a significantly increased number of wrong signs (see Table 4). Remarkably, the Zuber & Hug basis set with a high-quality force field and all calculations with the aug-cc-pVDZ basis show excellent agreement with the aug-cc-pVTZ data (independently of the reference functional used). Also, the cc-pVDZ data shows the largest deviations from the reference data followed by the Zuber & Hug basis property calculations in combination with the Zuber & Hug force field. For the largest molecule, the helicene **5**, we used the aug-cc-pVDZ basis set for the calculation of the reference data. This is justified in view of the excellent results obtained for the aug-cc-pVDZ basis set for the smaller molecules **1**−**4**. In contrast with the smaller molecules, we now observe many more wrong signs (compare Table 5). However, when all the data in Tables 1−5 are compared, it is encouraging to note that the basis set by Zuber & Hug in combination with the aug-cc-pVTZ (aug-cc-pVDZ for **5**) force field appears to perform better the larger the molecule becomes, lending further support to the use of this small basis set in combination with a high-quality force field.

TABLE 4: Comparison of the Calculated Intensity Differences for Left and Right Circularly Polarized Light for the Different Basis Sets and Functionals for 4[a]

		functional/ aug-cc-pVTZ		comparison to B3LYP/ aug-cc-pVTZ	
functional	basis set	$\delta(I)$	no. of wrong signs	$\delta(I)$	no. of wrong signs
LDA	3-21++G(p)[b]	0.275	5	0.364	4
	3-21++G(p)[b,c]	0.109	3	0.265	2
	Sadlej	0.161	1	0.323	2
	cc-pVDZ	0.589	11	0.744	10
	cc-pVTZ	0.349	5	0.467	4
	aug-cc-pVDZ	0.150	0	0.303	3
	aug-cc-pVTZ			0.280	3
BLYP	3-21++G(p)[b]	0.309	7	0.484	8
	3-21++G(p)[b,d]	0.102	0	0.211	1
	Sadlej	0.217	4	0.402	3
	cc-pVDZ	0.608	9	0.791	8
	cc-pVTZ	0.334	4	0.467	3
	aug-cc-pVDZ	0.079	1	0.245	2
	aug-cc-pVTZ			0.219	1
B3LYP	3-21++G(p)[b]	0.341	8		
	3-21++G(p)[b,e]	0.113	1		
	Sadlej	0.109	1		
	cc-pVDZ	0.641	8		
	cc-pVTZ	0.336	2		
	aug-cc-pVDZ	0.072	0		

[a] Total number of vibrational modes is 39. For an explanation of the different quantities, see text. [b] Using a single polarization function with exponent 0.2 for hydrogens only, as suggested by Zuber and Hug.[19] [c] Using the LDA/aug-cc-pVTZ force field, see text. [d] Using the BLYP/aug-cc-pVTZ force field, see text. [e] Using the B3LYP/aug-cc-pVTZ force field, see text.

TABLE 5: Comparison of the Calculated Intensity Differences for Left and Right Circularly Polarized Light for the Different Basis Sets and Functionals for 5[a]

		functional/ aug-cc-pVDZ		B3LYP/ aug-cc-pVDZ	
functional	basis set	$\delta(I)$	no. of wrong signs	$\delta(I)$	no. of wrong signs
LDA	3-21++G(p)[b]	0.271	8	0.646	12
	3-21++G(p)[b,c]	0.098	2	0.595	10
	Sadlej	0.134	3	0.657	15
	cc-pVDZ	0.317	10	0.813	12
	aug-cc-pVDZ			0.639	12
BLYP	3-21++G(p)[b]	0.734	13	0.781	10
	3-21++G(p)[b,d]	0.092	4	0.202	7
	Sadlej	0.156	9	0.244	8
	cc-pVDZ	0.318	8	0.495	9
	aug-cc-pVDZ			0.256	7
B3LYP	3-21++G(p)[b]	0.717	9		
	3-21++G(p)[b,e]	0.088	1		
	Sadlej	0.127	2		
	cc-pVDZ	0.319	8		

[a] Total number of vibrational modes is 57. For an explanation of the different quantities, see text. [b] Using a single polarization function with exponent 0.2 for hydrogens only, as suggested by Zuber and Hug.[19] [c] Using the LDA/aug-cc-pVTZ force field, see text. [d] Using the BLYP/aug-cc-pVTZ force field, see text. [e] Using the B3LYP/aug-cc-pVTZ force field, see text.

V. Comparison to Experiment

In this section, to verify the adequacy of the use of the B3LYP/aug-cc-pVTZ computational level as a benchmark for our calculations, we will compare the simulated VROA spectra with recent experimental spectra[20,21] of three of the molecules in this study. The three molecules are (*S*)-methyloxirane (**1**), (*M*)-spiro[2,2]pentane-1,4-diene (**4**), and (*M*)-σ-[4]-helicene (**5**). We do not compare the experimental and theoretical data for

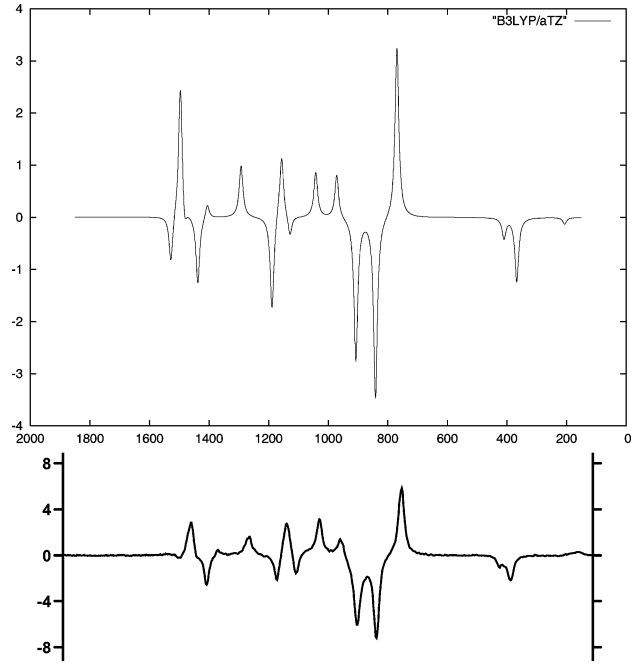

Figure 2. Theoretical (B3LYP/aug-cc-pVTZ, top) and experimental (bottom) intensity differences for backscattering VROA (${}^{n}I_{R}(\pi) - {}^{n}I_{L}(\pi)$) of (*S*)-methyloxirane, arbitrary units.

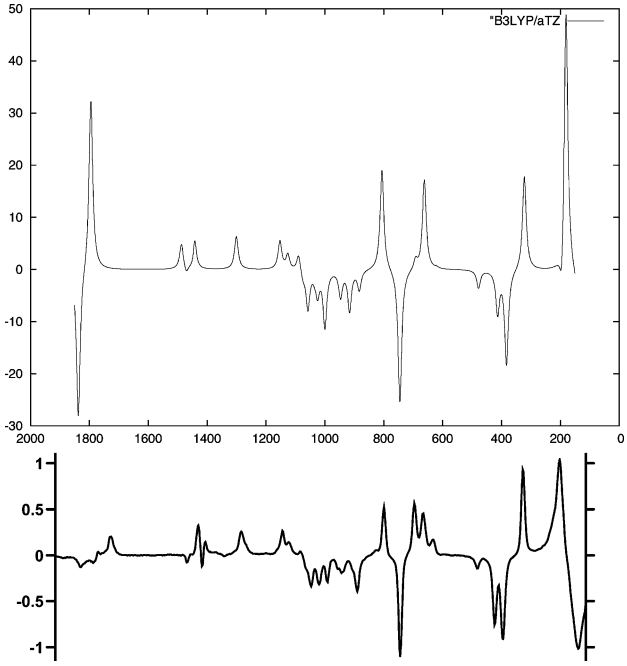

Figure 3. Theoretical (B3LYP/aug-cc-pVTZ, top) and experimental (bottom) intensity differences for backscattering VROA (${}^{n}I_{R}(\pi) - {}^{n}I_{L}(\pi)$) of (*M*)-spiro-[2,2]pentane-1,4-diene, arbitrary units.

(*R*)-epichlorhydrin (**2**) and (*S*)-glycidol (**3**), as these molecules have several conformational minima, and a proper Boltzmann averaging over the different structures would be required in order to reproduce the experimental data. All the simulated spectra have assumed a Lorenztian band shape with a bandwidth of 15 cm^{-1} and have been multiplied with the factor $(\omega - \omega_p)^4/(1 - \exp[-\hbar\omega_p/kT])$ without the speed of light *c*.

In Figure 2 we report the simulated spectrum for **1** calculated using B3LYP and the aug-cc-pVTZ basis set as well as the experimentally recorded spectrum. The agreement between experiment and this selected theoretical level is extraordinary good. With the exception of the very weak structure at about 206 cm^{-1}, all signs of the intensity differences agree between theory and experiment. A few differences in the relative intensities do exist, such as the two peaks at 1042 and 1128 cm^{-1}, as well as a few small off-sets in the vibrational frequencies, but the overall features of the experimental spectrum are very well reproduced, and the absolute configuration can be determined unambiguously. As such, the use of the B3LYP/aug-cc-pVTZ results as a benchmark appear well justified.

In Figure 3 we report the simulated and experimental spectrum for **4**. This molecule was recently synthesized by de Meijere et al.,[45] and the VROA spectrum of this molecule was recently recorded by Hug.[46] Whereas the overall features of the experimental VROA spectrum also in this case are well reproduced, the deviations are much larger between theory and the experiment for this molecule. The overall structure of the VROA spectrum is well reproduced for bands at shorter wavenumbers than 500 cm^{-1}. However, the fine structure of the bands between 650 and 700 cm^{-1} is missing, with only one of the vibrational bands having significant intensity. The theoretical spectrum shows several negative bands between 900 and 1000 cm^{-1}, whereas this fine structure is not evident from the experimental data. The small negative feature at about 1450 cm^{-1} in the experimental spectrum is not visible in the theoretical spectrum. However, the theoretical spectrum grossly exaggerates the VROA intensity differences around 1800 cm^{-1}.

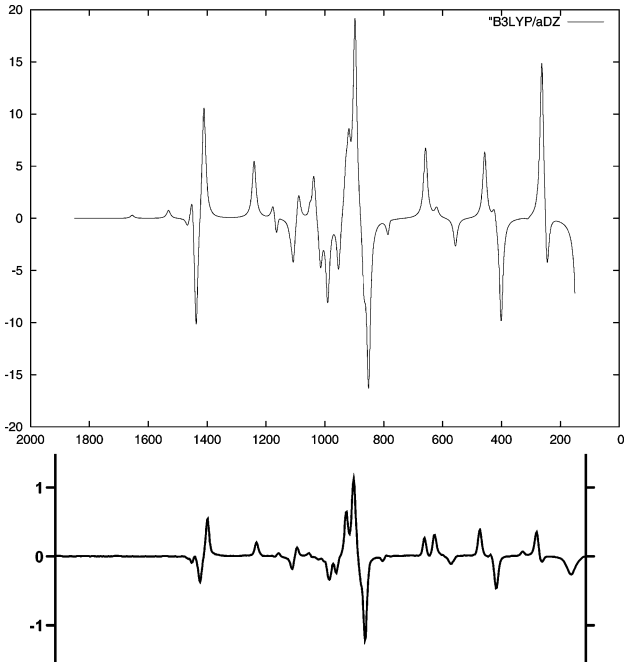

Figure 4. Theoretical (B3LYP/aug-cc-pVDZ, top) and experimental (bottom) intensity differences for backscattering VROA (${}^{n}I_{R}(\pi) - {}^{n}I_{L}(\pi)$) of (*M*)-$\sigma$-[4]-helicene. Arbitrary units.

Clearly, the B3LYP/aug-cc-pVTZ level does not fully match the experimental spectrum. However, these differences may not only arise from limitations in the computational model but also arise from the lack of anharmonic contributions as well as solvent effects in the theoretical calculations. Still, the absolute configuration of the molecule is easily determined from the predicted theoretical spectrum.

Finally, in Figure 4, we show the theoretical and experimental spectrum for **5**. As for **4**, the general structure of the spectrum is clearly reproduced by the theoretical calculations. However, it is important to realize that for this molecule, only the aug-cc-pVDZ basis set was used, and thus the force field may be

expected to be of poorer quality than that in the case of molecules **1** and **4**. This is also reflected in the spectrum. The weak structure at about 310 cm^{-1} has the opposite sign of that from the experiment. The band at 620 cm^{-1} in the theoretical spectrum appears to be much too weak compared to that from the experimental results. In the theoretical spectrum, there are several close-lying vibrations at about 1050 cm^{-1} with different signs, leading overall to a rather large, positive intensity difference feature, whereas in the experimental spectrum these bands give rise instead primarily to a very small, fine structure.

However, whereas differences between our "benchmark" theoretical data and the experimentally recorded spectra do exist, the agreement still has to be considered very satisfactory considering that no account has been made for solvent effects, nor of any anharmonic contributions, as well as inherent errors in our calculations. The agreement between the vibrational frequencies calculated using B3LYP/aug-cc-pVT(D)Z with the experimental results is overall very good—and in particular the ordering of the vibrational modes—allowing for an easy and direct comparison between theory and experiment.

VI. Concluding Remarks

In this study, we have conducted a systematic investigation of the role of basis set and density functional in the calculation of scattering intensity differences between left and right circularly polarized light (detection of the backscattered light). In general, we observe comparably good results for the aug-cc-pVDZ and aug-cc-pVTZ basis sets. The density functionals BLYP and B3LYP yield comparable results, while deviations are larger with LDA. It can thus be recommended to use gradient-corrected functionals, while the inclusion of the exact exchange is not essential. An important finding is thus that one may use gradient-corrected pure functionals such as BLYP for accurate VROA calculation, for which density fitting techniques can be used to speed up the calculations.[47]

Our results confirm that the small basis set proposed by Zuber and Hug is indeed able to reproduce the intensity differences with sufficient accuracy. A reason for this fortunate behavior might be the fact that errors introduced through the small basis set for absolute scattering intensities of left and right polarized light are likely to cancel upon subtraction in such a way that the scattering intensity differences depend only little on the size of the basis set provided that essential features are present in the basis (which means the diffuse polarization function on the hydrogen atoms, as also illustrated by Wiberg et al. in the context of optical rotation calculations[48]). The molecular structure and the harmonic force field used for the determination of the normal coordinates need to be calculated with a large basis set of, say, triple-ζ quality.

After more evidence was found for the remarkable accuracy of the small basis set by Zuber and Hug, larger molecules could now be studied by combining an accurate force field with this small basis for the calculation of the property tensors, whose geometric derivative yields the intensity differences. Consequently, we are currently investigating VROA for amino acids and small peptide molecules in combination with the selective calculation of characteristic modes via mode tracking,[43,44] in order to test for empirical rules that may connect the sign of the intensity differences with the structure and stereochemistry of the peptides, as well as theoretically study the VROA intensity differences arising from secondary structures of the polypeptides.

Acknowledgment. This work has been supported by DAAD (program PPP-Norwegen). K.R. has been supported by the Norwegian Research Council through a Strategic University Program in Quantum Chemistry (Grant No.154011/420) and an YFF Grant (Grant No. 162746/V00) as well as through an allocation of computer time provided by the Program for Supercomputing. This work has also received support through the COST-D26 program, including a STSM scholarship to V.L. M.R. has been supported by a Dozentenstipendium of the Fonds der Chemischen Industrie. V.L. thanks the FNRS for a Research Fellow position. A grant of computer time from Interuniversity Scientific Computation Facility is also gratefully acknowledged. We are grateful to Prof. W. Hug for providing us with the experimental spectra reproduced in this paper.

References and Notes

(1) Barron, L. D.; Buckingham, A. D. *Mol. Phys.* **1971**, *20*, 1111.
(2) Barron, L. D.; Bogaard, M. P.; Buckingham, A. D. *J. Am. Chem. Soc.* **1973**, *95*, 603.
(3) Hug, W.; Kint, S.; Bailey, G. F.; Scherer, J. R. *J. Am. Chem. Soc.* **1975**, *97*, 5589.
(4) See the company homepage at http://www.btools.com.
(5) Hug, W., Ed. In *Encyclopedia of Spectroscopy and Spectrometry*; Academic Press: London, 2000.
(6) Polavarapu, P. L. *J. Phys. Chem.* **1990**, *94*, 8106.
(7) Helgaker, T.; Ruud, K.; Bak, K. L.; Jørgensen, P.; Olsen, J. *Faraday Discuss.* **1994**, *99*, 165.
(8) London, F. *J. Phys. Radium* **1937**, *8*, 397.
(9) Ruud, K.; Helgaker, T.; Bour, P. *J. Phys. Chem. A* **2002**, *106*, 7448.
(10) Polavarapu, P. L. *Angew. Chem., Int. Ed.* **2002**, *41*, 4544.
(11) Macleod, M. A.; Butz, P.; Simons, J. P.; Grant, G. H.; Baker, C. M.; Tranter, G. E. *Phys. Chem. Chem. Phys.* **2005**, *7*, 1432.
(12) Pecul, M.; Ruud, K. *Int. J. Quantum Chem.* **2005**, *104*, 816.
(13) Nafie, L. A. *Annu. Rev. Phys. Chem.* **1997**, *48*, 357.
(14) Barron, L. D.; Hecht, L.; McColl, I. H.; Blanch, E. W. *Mol. Phys.* **2004**, *102*, 731.
(15) Liégeois, V.; Quinet, O.; Champagne, B. *J. Chem. Phys.* **2005**, *122*, 214304.
(16) Pecul, M.; Ruud, K. *Adv. Quantum Chem.* **2005**, *50*.
(17) Polavarapu, P. L. *Chirality* **2002**, *14*, 768.
(18) Stephens, P. J.; Devlin, F. J.; Cheeseman, J. R.; Drisch, M. J.; Bortolini, O.; Besse, P. *Chirality* **2003**, *15*, S57.
(19) Zuber, G.; Hug, W. *J. Phys. Chem. A* **2004**, *108*, 2108.
(20) Hug, W.; Zuber, G.; de Meijere, A.; Khlebnikov, A. F.; Hansen, H. J. *Helv. Chim. Acta* **2001**, *84*, 1.
(21) Hug, W. Personal communication.
(22) Placzek, G. *Handb. Radiologie* **1934**, *6* (2), 205.
(23) Epstein, S. T. *J. Chem. Phys.* **1965**, *42*, 2897.
(24) Barron, L. D. *Molecular Light Scattering and Optical Activity*; Cambridge University Press: Cambridge, U.K., 1982.
(25) Slater, J. C. *Phys. Rev.* **1951**, *81*, 385.
(26) Vosko, S. H.; Wilk, L.; Nusair, M. *Can. J. Phys.* **1980**, *58*, 1200.
(27) Becke, A. D. *Phys. Rev. A* **1988**, *38*, 3098.
(28) Lee, C.; Yang, W.; Parr, R. G. *Phys. Rev. B* **1988**, *57*, 785.
(29) Becke, A. D. *J. Chem. Phys.* **1993**, *98*, 5648.
(30) Dunning, T. H., Jr. *J. Chem. Phys.* **1989**, *90*, 1007.
(31) Kendall, R. A.; Dunning, T. H., Jr.; Harrison, R. J. *J. Chem. Phys.* **1992**, *96*, 6769.
(32) Sadlej, A. J. *Collect. Czech. Chem. Commun.* **1988**, *53*, 1995.
(33) Sadlej, A. J. *Theor. Chim. Acta* **1991**, *79*, 123.
(34) Clark, T.; Chandrasekhar, J.; Spitznagel, G. W.; Schleyer, P. v. R. *J. Comput. Chem.* **1983**, *4*, 294.
(35) Bose, P. K.; Barron, L. D.; Polavarapu, P. L. *Chem. Phys. Lett.* **1989**, *155*, 8106.
(36) Bose, P. K.; Polavarapu, P. L.; Barron, L. D.; Hecht, L. *J. Phys. Chem.* **1990**, *94*, 1734.
(37) Bak, K. L.; Devlin, F. J.; Ashvar, C. S.; Taylor, P. R.; Frisch, M. J.; Stephens, P. J. *J. Phys. Chem.* **1995**, *99*, 14918.
(38) Helgaker, T.; et al. *Dalton, an ab initio electronic structure program, Release 1.2*. http://www.kjemi.uio.no/software/dalton/dalton.html, 2001.
(39) Olsen, J.; Bak, K. L.; Ruud, K.; Helgaker, T.; Jørgensen, P. *Theor. Chim. Acta* **1995**, *90*, 421.
(40) Norman, P.; Jonsson, D.; Ågren, H.; Dahle, P.; Ruud, K.; Helgaker, T.; Koch, H. *Chem. Phys. Lett.* **1996**, *253*, 1.
(41) Ruud, K.; Wilson, D. J. D.; Salek, P.; Helgaker, T. In preparation.
(42) Neugebauer, J.; Reiher, M.; Kind, C.; Hess, B. A. *J. Comput. Chem.* **2002**, *23*, 895.
(43) Reiher, M.; Neugebauer, J. *J. Chem. Phys.* **2003**, *118*, 1634.
(44) Reiher, M.; Neugebauer, J. *Phys. Chem. Chem. Phys.* **2004**, *6*, 4621.

(45) de Meijere, A.; Khlebnikov, A. F.; Kozhushkov, S. I.; Kostikov, R. R.; Schreiner, P. R.; Wittkopp, A.; Rinderspracher, C.; Yufit, D. S.; Howard, J. A. K. *Chem. −Eur. J.* **2002**, *8*, 828.
(46) Hug, W. Unpublished work.
(47) Vahtras, O.; Almlöf, J.; Feyereisen, M. W. *Chem. Phys. Lett.* **1993**, *213*, 514.
(48) Wiberg, K. B.; Wang, Y.-G.; Vaccaro, P. H.; Cheeseman, J. R.; Trucks, G.; Frisch, M. J. *J. Phys.* Chem. *A* **2004**, *108*, 32.